Monitoring Atomic Cluster Expansion by High-Harmonic Generation

Vasily Strelkov,[1,2] Ulf Saalmann,[2,3] Andreas Becker,[2,4] and Jan M. Rost[2,3]

[1]*General Physics Institute of the Russian Academy of Sciences, Vavilova street 38, Moscow 119991, Russia*
[2]*Max Planck Institute for the Physics of Complex Systems, Nöthnitzer Straße 38, 01187 Dresden, Germany*
[3]*Max Planck Advanced Study Group at the CFEL, Luruper Chaussee 149, 22761 Hamburg, Germany*
[4]*JILA and Department of Physics, University of Colorado, Boulder, Colorado 80309-0440, USA*

(Received 4 December 2010; published 9 September 2011)

High-harmonic generation is shown to be capable of providing time-resolved information about the particle density of a complex system. As an example, we study numerically high-harmonic generation from expanding xenon clusters in a pump-probe laser scheme, where the pump laser pulse induces the cluster explosion and the probe pulse generates harmonics in the expanding cluster. We show that the high-harmonic spectra characterize the properties of the expanding cluster. Hence, measuring the dependence of the harmonic signal on the pump-probe delay suggests itself as an experimental tool to monitor many-particle dynamics with unique temporal resolution; based on optical measurements, this technique is naturally free from any spatial charge effects.

DOI: 10.1103/PhysRevLett.107.113901 PACS numbers: 42.65.Ky, 32.80.Rm, 36.40.Sx, 36.40.Wa

High-harmonic generation (HHG) is based on a simple yet nontrivial mechanism, today also known as the three-step model [1,2]. It describes HHG as result of tunneling ionization of the generating atom or ion by the laser field, free electronic motion in this field, and recombination accompanied by the XUV emission upon the return to the parent ion. Now HHG has evolved to a versatile tool which even paved the way to the generation of attosecond pulses [3,4]. HHG also opens a perspective on imaging microscopic distances such as the bond length of molecules [5,6] or, under certain circumstances, molecular electronic orbitals [7,8]. While these are detailed properties of small systems, here we are interested in obtaining microscopic yet robust information on properties of complex systems which change on a femtosecond time scale, e.g., the mean particle density in a complex system.

A prototypical example is a rare-gas cluster which contains many atoms that eventually become charged during irradiation with a strong laser pulse [9]. As a consequence, the cluster undergoes Coulomb explosion which lowers its density on a femtosecond time scale. HHG emitted from clusters has been studied extensively [10–14], but not with the intention to monitor time-dependent properties of the cluster. A scenario [15], which comes close to the one we propose here, is the irradiation of xenon clusters with two high-intensity femtosecond laser pulses, one at the laser fundamental frequency and one at its second harmonic. In this experiment the ion energies from the exploding xenon clusters were measured. Note that electronic or ionic spectra used to characterize cluster expansion can be affected by the macroscopic quasistatic electric field appearing in a cluster jet irradiated by an intense laser field. Therefore we suggest an optical measurement that is free from this drawback. Moreover, the harmonics characterize the medium at the instant of the irradiation by the probe pulse and thus are not affected by its further dynamics.

We consider a pump-probe scenario, such that a first pulse at 780 nm ionizes almost all atoms in the cluster to the first or even higher charge state. This pulse, therefore, initiates the time-dependent evolution of the cluster, while the second one at 390 nm ''stops'' the clock emitting the high harmonics. It is chosen sufficiently weak (regarding duration and intensity) to keep photoionization to even higher charge states and cluster expansion during the probe pulse negligible. The harmonics in the region of the HH plateau (with frequencies ω_n larger than the ionization potential of an ion in the system) correspond to long (dozens of Bohr radii) electronic excursion orbits before the recombination with the ion. As we will demonstrate below, they naturally scan the environment of the ions in the cluster, which allows one to image the averaged particle density and the static field of the cluster. With a variable delay τ between the two pulses, time-resolved information about the particle density of the exploding cluster is monitored.

To be specific we will consider Xe_{135} in icosahedral ground state geometry [16]. This symmetry is not important; Xe_{134} with a completely different ground state geometry produces a very similar HHG response. We use a quasiclassical approach [17,18] for the time-dependent cluster evolution which includes ionization and cluster expansion induced by the pump pulse. From this calculation ionic charge states, ionic positions, and the spatial distribution of ionized electrons are known at each instant of time. For the present parameters of the pump pulse, almost all cluster atoms are ionized with charges ranging from 1 to 3. The high-harmonic spectrum of the expanding cluster, generated by the second laser pulse, is determined by numerically solving the time-dependent Schrödinger

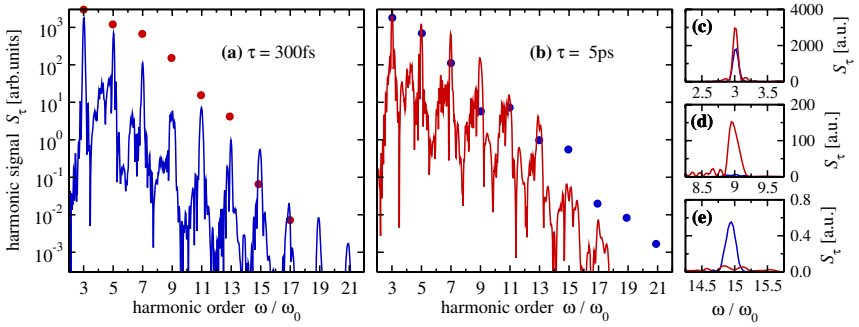

FIG. 1 (color online). Harmonic spectra generated by the probe pulse in an expanding Xe_{135} cluster and scaled in units of the probe frequency ω_0. The pump-probe delays (i.e., the expansion times) are $\tau = 300$ fs (a) (blue line) and 5 ps (b) (red line). For comparison we show the peak positions for the 5 ps probe as circles in (a) and, similarly, the one for 300 fs probe in (b). The expansion is pumped with a 780 nm, 25 fs-long laser pulse with a peak intensity of 1.3×10^{14} W/cm^2. The wavelength of the probe pulse is 390 nm, its duration is 10 fs, and the intensity is 1.5×10^{14} W/cm^2. The three insets show individual lines for the harmonic orders $n = 3$ (c), $n = 9$ (d), and $n = 15$ (e) on a linear scale.

equation (TDSE) for a single active electron bound to an ion [19] and exposed to an additional external field given by the probe pulse and the Coulomb field generated by all the ions and the electron density inside the cluster. We note that the effect of the electrons decreases with increase of the pump-probe time delay and is, in general, negligible. Binding of an electron to an ion of charge $Z + 1$ is described by a "soft Coulomb" potential $V_Z(\mathbf{r}) = -(Z + 1)/\sqrt{a_Z^2 + r^2}$, where a_Z is chosen to give the correct ionization potential for the xenon ion with charge state Z. Since the external field varies with the position of the respective ion inside the cluster, the TDSE is solved and the time-dependent dipole is evaluated for each of the 135 ions of the cluster. The spectrum of radiation emitted by the cluster is calculated by coherently summing the individual ionic contributions from all ions [20]. Finally, the results from different initial cluster orientations are averaged.

The present single active electron approach is applicable for a dilute medium, i.e., for large mean distance a from a particle to its nearest neighbor. Many-electron effects have been shown to be negligible for a linear chain of atoms if $a \geq 5$ Å [21], which is the case in our situation.

The spectral intensities $S_\tau(\omega)$ emitted from an exploding Xe_{135} cluster for two expansion times τ are presented in Fig. 1, where τ is defined as the delay between the maxima of the two pulses. The spectrum does not exhibit the usual plateau structure known, e.g., for harmonics generated from atoms at midinfrared fields [22], due to the short wavelength of the probe pulse and the overlapping contributions from ions of the first three charge states with different cutoffs, $n_Z\omega_0 = E_Z + 3.17U_p$ at $n_1 = 9$, $n_2 = 13$, and $n_3 = 15$ [1,2]. Here, E_Z is the ionization energy of the ion of charge state Z and $U_p = F^2/(4\omega_0^2)$ is the ponderomotive energy in the laser field of frequency ω_0 and peak strength F. The two spectra in Fig. 1, taken at intermediate [300 fs, blue solid line in 1(a)] and long [5 ps, red solid line in 1(b)] expansion times, differ significantly. The intensities of the low and intermediate harmonics are weaker at $\tau = 300$ fs than at the end of the expansion $\tau = 5$ ps; for the higher harmonics ($n \geq 15$) it is just the opposite.

The harmonic emission is determined, on one hand, by the number and the charge state of the ions contributing to the signal and, on the other hand, by the ion density. For the analysis we have calculated the total yield of the nth harmonic as an integral of the spectral intensity:

$$I_n(\tau) = \int_{n\omega_0-\delta\omega}^{n\omega_0+\delta\omega} d\omega S_\tau(\omega). \quad (1)$$

For the integration range we have chosen $\delta\omega = 0.3\omega_0$.

The high harmonics are sensitive to the ionic density since their generation involves free electronic wave packet oscillation over dozens of Bohr radii. The Coulomb field of the surrounding ions causes a dephasing of the wave packet and results in a loss of coherence of the many-particle harmonic response. The dephasing disappears as the medium density decreases below a critical value [20], which we call threshold density ρ_n for harmonic n. They are defined as ionic densities at which the signal of the harmonic is only 50% of its low-density limit. The transition can be seen in Fig. 2(a), in which we present the normalized signals

$$J_n(\tau) = I_n(\tau)/I_n^\infty, \quad (2)$$

of the 7th, 9th, and 11th harmonic. I_n^∞ is the coherent sum of spectra from isolated ions. This sum corresponds to the signal emitted by the cluster at the final stage of its expansion when the interionic distances are so large that the HHG of each ion is not affected by the fields of the surrounding ions. The normalized signals found with Eq. (2) show a rapid increase as a function of the pump-probe delay, followed by their saturation at long expansion

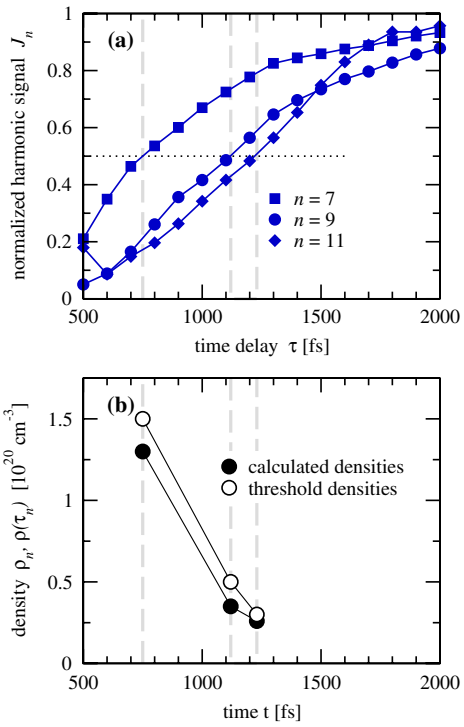

FIG. 2 (color online). (a) Normalized harmonic signals ($n = 7, 9, 11$) from Xe_{135} found with Eqs. (1) and (2) as a function of the time delay τ between pump and probe pulses; the parameters are the same as in Fig. 1. (b) Comparison of the densities calculated in the cluster simulation (filled circles) for the times (gray vertical lines) when the 50% level is reached and the threshold densities (open circles) for these harmonics; see text for details.

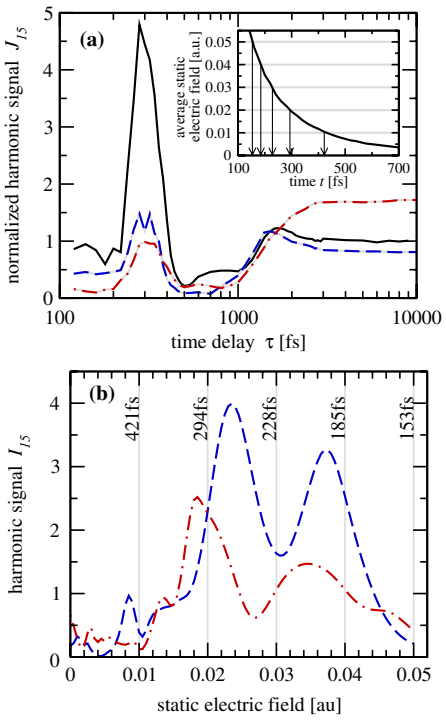

FIG. 3 (color online). (a) Normalized signal J_{15} of the 15th harmonic (black line) emitted by the cluster Xe_{135} (same laser pulse parameters as in Fig. 1) as a function of the time delay τ between pump and probe pulse. Contributions from Xe^{2+} (dashed blue line) and Xe^{3+} (dot-dashed red line) ions are shown separately. Inset: Average electric field (due to the other ions in the cluster) seen by the ions as a function of time τ. (b) Harmonic signal I_{15} for Xe^{2+} (dashed blue line) and Xe^{3+} (dot-dashed red line) ions in the presence of a static electric field. The times at the vertical gray lines indicate at which time during the cluster expansion the corresponding electric field acts on the cluster ions, cf. the arrows in the inset of (a).

times, in agreement with our interpretation above. The threshold densities of $\rho_7 = 1.5 \times 10^{20}$ cm^{-3}, $\rho_9 = 5 \times 10^{19}$ cm^{-3}, and $\rho_{11} = 3 \times 10^{19}$ cm^{-3}, obtained using a technique developed previously [20], agree very well with the averaged ionic densities $\rho(\tau_7) = 1.3 \times 10^{20}$ cm^{-3}, $\rho(\tau_9) = 3.5 \times 10^{19}$ cm^{-3}, and $\rho(\tau_{11}) = 2.6 \times 10^{19}$ cm^{-3} calculated at the corresponding transition times τ_n marked in Fig. 2. Thus, an experimental observation of the harmonic signal as a function of the pump-probe delay allows one to reconstruct the time evolution of the density in the exploding cluster as following: delays τ_n corresponding to the 50% level of the harmonic signal are found for different harmonics, and the densities for these delays are approximated by the threshold densities ρ_n.

Next, in Fig. 3(a) we present the normalized signal of one of the highest harmonics, namely, the 15th harmonic, as a function of the cluster expansion time. It exhibits a clear maximum around $\tau = 280$ fs. Studying separately the contributions from the different ionic states we find that the 15th harmonic is generated mainly by Xe^{2+} (dashed blue line) and Xe^{3+} ions (dot-dashed red line), both exhibiting a maximum too.

The characteristic maximum in the harmonic signal can be attributed to the (radial) quasistatic electric field inside a charged cluster, which decreases steadily as the cluster expands, cf. inset in Fig. 3(a). It is known that a weak static electric field can enhance the harmonic signal significantly [23–25]; this enhancement is attributed, first, to the ionization enhancement, and, second, to the modification of the electronic trajectories in the continuum. In order to study the expectation about the effect of the static cluster field on the harmonic signal shown in Fig. 3(a), we have calculated the intensity of the 15th harmonic generated by isolated Xe^{2+} and Xe^{3+} ions in the presence of a static field E_{stat} parallel to the probe field. The corresponding results are shown in Fig. 3(b) as a function of E_{stat}. Both signals are at maximum for static field strengths of about 0.02–0.04 a.u., which agrees well with the average field strengths at about 200–300 fs in the expanding cluster indicated by the vertical lines in Fig. 3(b). We note that the maximum of the harmonic yield from the Xe^{2+} and the Xe^{3+} ions around $\tau = 300$ fs can be related to the maximal emission at external fields of about 0.02 a.u., cf. Figs. 3(a) and 3(b). Such strong influence of the static field is typical

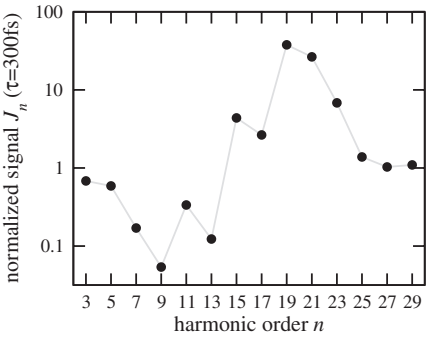

FIG. 4. Normalized signal J_n of the nth harmonic emitted by the cluster Xe_{135} at a time delay of 300 fs. Laser parameters are the same as in Fig. 1.

for harmonics close to and beyond the cutoff because in the presence of a static electric field there are classical electronic trajectories coming back to the origin with energies exceeding $3.17U_p$ leading to a shift of the cutoff to higher frequency [24]. In the cluster response we have also found such a pronounced enhancement for the other highest harmonics ($n > 15$). This can be seen from the normalized signals J_n of the individual harmonics obtained at a time delay of 300 fs, shown in Fig. 4.

Note that study of the quasistatic electric field in the expanding cluster with this technique could be very useful in the case of an *anisotropic* cluster expansion, recently observed experimentally [26]. In this case the harmonic signal should depend strongly on the relative direction of the probe polarization and the direction of the cluster expansion. Indeed, when they are parallel to each other the harmonic is enhanced due to the above-mentioned mechanism. On the contrary, under perpendicular directions the free electronic wave packet drifts due to the static field and thus misses the parent ion which suppresses HHG.

The dynamics of the cluster explosion is size dependent. Thus, the time instants at which the threshold densities are reached will vary with the cluster size. We therefore propose to study cluster expansion in experiments with mass-selected cluster beams. The mass selection results in a very dilute cluster beam. However, results of successful experiments using such beams have been reported recently [27,28]. We note that observation of the threshold densities does not require high HHG efficiency and thus it is possible using dilute cluster beams. Moreover, using a low-density target and a probe pulse at short wavelengths, as in the present numerical study, experimentally helps to avoid detuning from the phase matching, which could otherwise impact the observation of the threshold densities. Note that in a typical high harmonics experiment the spatial intensity profile often leads to a convolution of the harmonic signals; however, laser beams with a flattop intensity profile may help to reduce the impact of the profile effect (see, e.g., [29,30]). Finally, HHG via long-range electron transfer [31] is negligible in our simulations because it assumes densities well above the threshold density; however, for different conditions this might not be the case.

In conclusion, we have shown that high-harmonic generation is an effective tool to monitor atomic cluster expansion and provide temporal information about the particle density in such a complex many-body system. This has been exemplified by numerical simulations of Xe clusters interacting with two ultrashort laser pulses, where the pump pulse initiates the temporal dynamics, namely, the charging and explosion of the cluster, and the time-delayed probe pulse generates the harmonics in the expanding cluster. In particular, the higher harmonics scan the environment of the individual ions revealing the time-dependent particle density and average static field in the expanding cluster.

V. S. acknowledges the hospitality of the Max Planck Institute for the Physics of Complex Systems, as well as financial support from RFBR and the Russian Ministry of Science and Education (MD-5752.2010.2). A. B. acknowledges partial support by the U.S. National Science Foundation.

[1] P. B. Corkum, Phys. Rev. Lett. **71**, 1994 (1993).
[2] K. J. Schafer, B. Yang, L. F. DiMauro, and K. C. Kulander, Phys. Rev. Lett. **70**, 1599 (1993).
[3] P. B. Corkum and F. Krausz, Nature Phys. **3**, 381 (2007).
[4] F. Krausz and M. Ivanov, Rev. Mod. Phys. **81**, 163 (2009)
[5] M. Lein, N. Hay, R. Velotta, J. P. Marangos, and P. L. Knight, Phys. Rev. Lett. **88**, 183903 (2002).
[6] M. Lein, Phys. Rev. Lett. **94**, 053004 (2005).
[7] J. Itatani *et al.*, Nature (London) **432**, 867 (2004).
[8] O. Smirnova *et al.*, Nature (London) **460**, 972 (2009).
[9] U. Saalmann, Ch. Siedschlag, and J. M. Rost, J. Phys. B **39**, R39 (2006).
[10] T. D. Donnelly, T. Ditmire, K. Neuman, M. D. Perry, and R. W. Falcone, Phys. Rev. Lett. **76**, 2472 (1996).
[11] J. W. G. Tisch *et al.*, J. Phys. B **30**, L709 (1997).
[12] C. Vozzi *et al.*, Appl. Phys. Lett. **86**, 111121 (2005).
[13] B. Shim, G. Hays, R. Zgadzaj, T. Ditmire, and M. C. Downer, Phys. Rev. Lett. **98**, 123902 (2007).
[14] H. Singhal *et al.*, J. Phys. B **43**, 025603 (2010).
[15] E. Springate *et al.*, Phys. Rev. A **61**, 044101 (2000).
[16] D. J. Wales *et al.*, http://www-wales.ch.cam.ac.uk/CCD.html.
[17] U. Saalmann and J. M. Rost, Phys. Rev. Lett. **91**, 223401 (2003).
[18] U. Saalmann, J. Mod. Opt. **53**, 173 (2006).
[19] V. V. Strelkov, A. F. Sterjantov, N. Yu Shubin, and V. T. Platonenko, J. Phys. B **39**, 577 (2006).
[20] V. V. Strelkov, V. T. Platonenko, and A. Becker, Phys. Rev. A **71**, 053808 (2005).
[21] V. Véniard, R. Taïeb, and A. Maquet, Phys. Rev. A **65**, 013202 (2001).
[22] J. Tate *et al.*, Phys. Rev. Lett. **98**, 013901 (2007).
[23] M.-Q. Bao and A. F. Starace, Phys. Rev. A **53**, R3723 (1996).

[24] B. Wang, X. Li, and P. Fu, Phys. Rev. A **59**, 2894 (1999).
[25] B. Borca *et al.*, Phys. Rev. Lett. **85**, 732 (2000).
[26] E. Skopalova *et al.*, Phys. Rev. Lett. **104**, 203401 (2010).
[27] O. Kostko, B. Huber, M. Moseler, and B. von Issendorff, Phys. Rev. Lett. **98**, 043401 (2007).
[28] C. Bartels *et al.*, Science **323**, 1323 (2009).
[29] E. S. Toma, Ph. Antoine, A. de Bohan, and H. G. Muller, J. Phys. B **32**, 5843 (1999).
[30] V. V. Strelkov, E. Mevel, and E. Constant, New J. Phys. **10**, 083040 (2008).
[31] A. D. Bandrauk, S. Barmaki, and G. L. Kamta, Phys. Rev. Lett. **98**, 013001 (2007).